

Application to argon ions of a new technique to measure the two-electron contribution to the ground state energy of helium-like ions

F J Currell[†]§, J Asada[‡], T V Back^{||}, C Z Dong[¶], H S Margolis⁺,
N Nakamura[§], S Ohtani[‡]§, J D Silver^{||} and H Watanabe[§]

[†] Atomic and Molecular Research Division, Department of Pure and Applied Physics, The Queen's University of Belfast, Belfast BT7 INN, UK

[‡] Institute for Laser Science, University of Electro-Communications, Chofu, Tokyo 182-8585, Japan

[§] Cold Trapped Ions Project, ICORP, JST, Axis Chofu 3F, 1-40-2 Fuda, Chofu, Tokyo 182-0024, Japan

^{||} Clarendon Laboratory, Department of Physics, University of Oxford, Parks Road, Oxford OX1 3PU, UK

[¶] Department of Physics, Northwest Normal University, Lanzhou 730070, People's Republic of China

⁺ National Physical Laboratory, Queens Road, Teddington TW11 0LW, UK

E-mail: f.j.currell@qub.ac.uk

Received 28 May 1999, in final form 4 November 1999

Abstract. We have measured the two-electron contribution of the ground state energy of helium-like argon ions using an electron beam ion trap (EBIT). A two-dimensional map was measured showing the intensity of x-rays from the trap passing through a krypton-filled absorption cell. The independent axes of this map were electron beam energy and x-ray energy. From this map, we deduced the two-electron contribution of the ground state of helium-like argon. This experimentally determined value (312.4 ± 9.5 eV) was found to be in good agreement with our calculated values (about 303.35 eV) and previous calculations of the same quantity. Based on these measurements, we have shown that a ten-day absorption spectroscopy run with a super-EBIT should be sufficient to provide a new benchmark value for the two-electron contribution to the ground state of helium-like krypton. Such a measurement would then constitute a test of quantum electrodynamics to second order.

1. Introduction

From their inception (Levine *et al* 1988) electron beam ion traps (EBITs) have been used for a variety of spectroscopic studies. Since the operation of these devices has been described elsewhere (Levine *et al* 1988) we will provide only a short summary here. Essentially, a high-current, high-energy electron beam is magnetically compressed. The resultant beam waist has a radius of typically $35 \mu\text{m}$. Radial trapping of positive ions occurs in the region of the beam waist due to the electron beam's space charge. Axial trapping is achieved with a series of cylindrical drift tubes. Hence, a trap region is created which traps all positive ions, provided their kinetic energies are sufficiently low (typically $10q$ eV for an ion of charge state q).

The actual abundance of various ion species in the trap is a complicated function of various machine and atomic physics parameters. A model has been created (Penetrante *et al* 1991,

Margolis *et al* 1997) which takes these parameters as inputs. The coupled rate equations are then solved to give predictions of the abundances of various charge states in the trap. Machine parameters used are the electrostatic trap depth, the magnetic field, the electron beam's energy and current and number densities of source neutral or low charge-state species. Atomic physics parameters are the cross sections for radiative recombination (RR), electron impact ionization and charge exchange for each charge state. This model shows that by careful selection of the machine parameters, it is possible to choose the charge balance so that one or two species dominate.

Various forms of spectroscopy have been performed on the ions trapped in an EBIT, with information about atomic physics, quantum electrodynamics (QED) and relativistic effects having been obtained. Solid-state detectors (SSDs) provide a simple method of obtaining the energies of transitions over a wide energy range, with high sensitivity, although the resolution is generally lower than with other methods.

Spectra from SSDs have been used to diagnose the charge balance of trapped ions (Margolis *et al* 1997), to deduce ionization cross sections (Marrs *et al* 1997) and to measure the binding energies of ions, among others. More specifically, the difference in binding energies of hydrogen-like and helium-like ions has been measured (Marrs *et al* 1995). This was achieved by measuring the splitting of two RR features. These features were due to capture into the ground state of bare and hydrogen-like ions. The energy of photons emitted during RR is the sum of the electron beam energy and the binding energy of the level into which the electron was captured. Accordingly, the difference in energies of the two RR features is equal to the difference in binding energies of the hydrogen-like and helium-like ion. This difference is a direct measure of the two-electron contribution of the ground state energy of the helium-like ion concerned and can offer a useful test of two-electron QED (Persson *et al* 1996).

A layer of absorbing material placed before a SSD offers a simple way of overcoming the inherent resolution limitations whilst retaining reasonable sensitivity for spectroscopy of RR features. Essentially, the absorber acts as a low-pass filter. Changing the electron beam energy can change the x-ray energy of any RR feature. The total detected x-ray yield decreases as the beam energy increases when a RR feature moves 'through' the absorption edge. This technique has been used to measure the energy spread of the electron beam of an EBIT (Levine *et al* 1989) and to determine intensities of RR peaks in order to determine L-shell electron-impact ionization cross sections (Stöhlker *et al* 1997). In contrast, we used an absorber to determine the difference in energies of nearby RR features. In order to improve the statistical quality, we measured a two-dimensional map, somewhat similar to those used for measuring dielectronic recombination spectra (see, for example, Knapp 1991 or Asada *et al* 1997).

Although not a test of QED, measurement of the two-electron contribution to the ground state of the helium-like argon ion is useful as a test of relativistic atomic structure codes and provides an assessment of the effects of electron correlation on medium- Z ions. Furthermore, such a measurement constitutes a good feasibility study for similar measurements on ions of higher charge where QED effects can be tested.

2. Method

The Oxford EBIT (Silver *et al* 1994) was tuned to produce an electron beam with an energy of 10 keV, at a current of 67 mA. A magnetic field of 2.7 T was used and the axial trap depth was set at 400 V. Argon gas was injected from a side port. X-rays were measured using a lithium-drifted silicon detector with a resolution of about 150 eV at 5.9 keV. The device was configured so that there were roughly one third as many bare argon ions as hydrogen-like ones. Under such conditions, a spectrum like that shown in figure 1 will be observed if no absorption

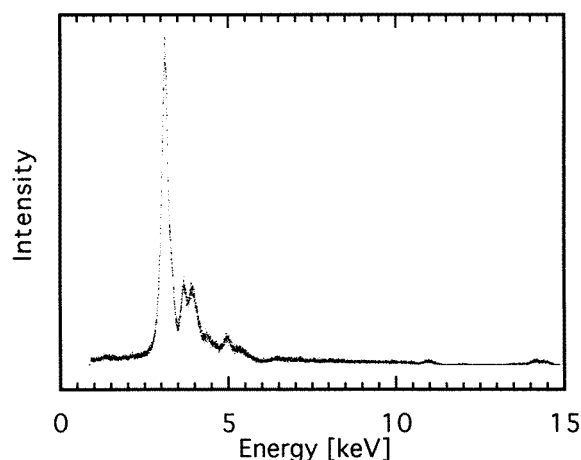


Figure 1. X-ray spectrum taken with a solid-state detector when Ar was injected into the EBIT. No absorber was used to attenuate the signal. The features of interest are the small peaks at about 14 keV x-ray energy. See text for details.

cell is placed between the detector and the trapped ions. There is some x-ray attenuation at low energies due to two thin beryllium windows used to ensure the vacuum quality. The radiative recombination features of interest are the weak features at about 14 keV x-ray energy.

A multiparameter data acquisition system (Currell *et al* 1997) was used to measure the energies of x-rays emitted as a function of electron beam energy. During the measurement, the electron beam energy was swept from about 9.6 to 10.4 keV by applying a 100 Hz ramp waveform to the input of a Trek 20/20 beam energy supply. Data collected during the up and down sweeps of the waveform were compared to confirm that the slew-direction had no effect on the EBIT operating conditions. Prior to detection, the x-rays passed through a 7 cm thick absorption cell filled with krypton at atmospheric pressure. A portion of the resultant data set is shown in figure 2. This figure shows the composite spectrum based on three separate runs. The total acquisition time was 20 h. Notice the intensities of the radiative recombination peaks decrease as the absorber attenuates them. For comparison, similar spectra were also collected with the absorption cell filled with nitrogen. When nitrogen was used, no attenuation was observed in this electron beam energy and x-ray energy region.

The x-ray energy scale was calibrated using ^{55}Fe and ^{57}Co radioactive isotope sources. The absolute electron beam energy was calibrated from the power-supply values and can be expected to have a large systematic error (about 50 V) due to effects such as the space-charge potential of the compressed electron beam. The channel spacing of the electron beam energy scale was derived by examining the shift of radiative recombination peaks as the beam energy was changed. The full procedure is described below.

3. Results and analysis

The two-electron contribution manifests itself in two different ways in a data set like figure 2. The horizontal spacing between the two diagonal features gives us the two-electron energy contribution as described by Marrs *et al* (1995). The statistical uncertainty derived from the horizontal spacing is related to the convolution of the detector resolution and the electron beam width (a total of about 250 eV). The beam energy at which a feature is attenuated is given by

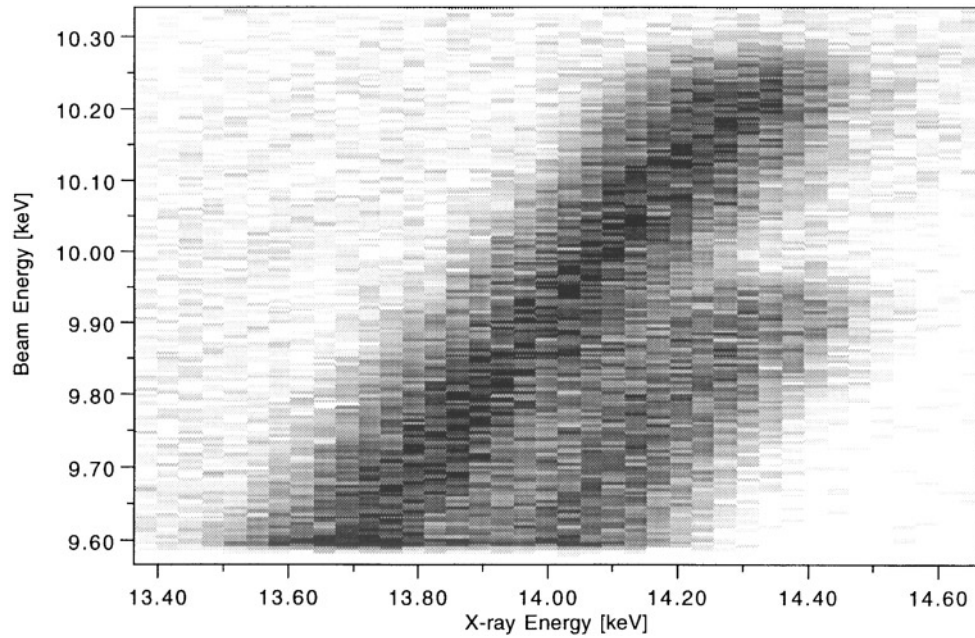


Figure 2. A two-dimensional map showing the number of detection events as a function of the electron beam energy and x-ray energy. These events are primarily due to photons emitted during radiative recombination, which then passed through a krypton absorption cell before reaching the solid-state detector. The attenuation of the signal at an energy of about 14.3 keV is due to the krypton absorption edge.

the difference between the binding energy into which an electron is captured and the energy of the absorption edge. Hence, the vertical spacing between the electron beam energies at which the two features are attenuated also gives the two-electron energy contribution. The characteristic width associated with this measurement is just that of the electron beam because the absorption edge in krypton is much narrower (Deutsch and Hart 1986). From the data shown in figure 2, we have derived the two-electron contribution in two separate manners.

For each slice (i.e. electron beam energy) of the data shown in figure 2, the two line-profiles observed were fitted to the function given in equation (1):

$$I(x; \Delta x, \bar{x}_1, h_0, h_1, c, \sigma) = h_0 \exp\left(-\frac{(x - \bar{x}_1 + \Delta x)^2}{2\sigma^2}\right) + h_1 \exp\left(-\frac{(x - \bar{x}_1)^2}{2\sigma^2}\right) + c. \quad (1)$$

The independent variable x represents the x-ray energy scale. All other parameters (written after the semicolon) are parameters determined by fitting. One value was used for σ , the widths of the peaks, for the whole data set, all other parameters were independently determined for each electron energy (i.e. slice of the data set). Parameters with a subscript i (equal to 0 or 1) relate to the feature due to radiative recombination into an ion with i electrons. Hence, h_0 is the height of the RR peak due to capture by bare Ar and h_1 is the height of the RR peak due to capture by hydrogen-like Ar. The position of the RR peak due to capture by bare Ar was not represented as a single parameter \bar{x}_0 but was instead represented by the difference between the two peaks, Δx , and the position of the RR peak into hydrogen-like Ar, \bar{x}_1 . Representing the spectrum in this way is advantageous for subsequent error analysis since the parameter Δx directly gives the two-electron energy contribution of interest. The constant c was included to account for a small energy-independent background. Fitting was achieved using the Marquardt

method as described by Press *et al* (1992).

Each fit to one slice (i.e. one-electron beam energy) of the data yields an estimate of the two-electron energy contribution from the parameter Δx . The weighted mean of all the separate values of Δx was calculated. The weights were derived from the fit described above. This yielded a value of 292 ± 31 eV for the two-electron contribution to the ground state energy. This measurement is analogous to the measurement described by Marrs *et al* (1995) although a different fitting function has been used. The statistical precision when using the absorber (all other factors being equal) is somewhat worse since the count rate is reduced. This reduction in count rate is about a factor of two.

The advantage of the method we have used here compared with that of Marrs *et al* (1995) is that the two-electron contribution is represented in the data in a second independent way as described above. The electron beam energy at which an RR peak is attenuated is given by the difference between the energy of the absorption edge and the binding energy of the capture level. Hence, the difference between two attenuation energies gives the two-electron contribution.

The energy of an RR peak is equal to the sum of the electron beam energy and the binding energy of the orbital into which the electron is captured. Accordingly, the relative electron beam energy scale was derived from the variation of \bar{x}_1 with electron energy. A least-squares fit to a straight line was performed to determine the change of \bar{x}_1 as a function of beam energy as measured by the multiparameter system. The slope of the line then gave the relative electron beam energy scale E , used in figure 2.

The two 'spectra' $h_0(E)$ and $h_1(E)$ deduced from the first fitting procedure were then analysed to give a second measurement of the two-electron contribution. These two spectra are shown in figure 3. We fitted the data by assuming $h_0(E)$ and $h_1(E)$ had the same unknown functional form with an unknown intensity ratio A . It is safe to make this assumption since the RR cross sections are slowly varying functions of energy. Hence the two profiles are both the convolution of the electron beam energy distribution and the absorption profile and so are expected to have the same shape but differ in intensity. Compared with fitting the line profiles to some function (e.g. an error function), our procedure has the advantage that no assumptions are made about the energy distribution of the electron beam.

We calculated the chi-squared for various shifts of the two intensity distributions (d , an integer number of data channels). For each value of d , we minimized the chi-squared as a function of A . In the region where chi-squared goes to a minimum, it has a parabolic form when plotted as a function of d . From the values of chi-squared near to this minimum, we determined the smallest value of d (d_{\min} , a non-integer) and the statistical uncertainty associated with d_{\min} .

We converted d_{\min} to a difference in beam energy (ΔE) using the beam energy scale derived previously. This gave us a result of 314.5 ± 10 eV for the two-electron energy contribution. Since this quantity is derived from the differences of two energies, the systematic error in the energy scale cancels. All but about 1.5 eV of this error comes from the error in the slope used to derive the electron beam energy scale. The remaining 1.5 eV arises from the statistical uncertainties in the peak intensities.

Although they are derived from the same data set, our two measurements of the two-electron contribution are statistically independent. This can be seen from the fact that no parameters from the fit to equation (1) are common to both determinations. We can combine the two measured values to give a weighted mean of 312.4 ± 9.5 eV although this is only a small improvement on the value taken from the absorption edge technique alone.

To arrive at a theoretical value for comparison, we calculated the orbital energies of 1s electrons in the ground states of Ar^{16+} and Ar^{17+} . Taking the difference between these two calculated orbital energies then yielded a theoretical estimate for the two-electron contribution

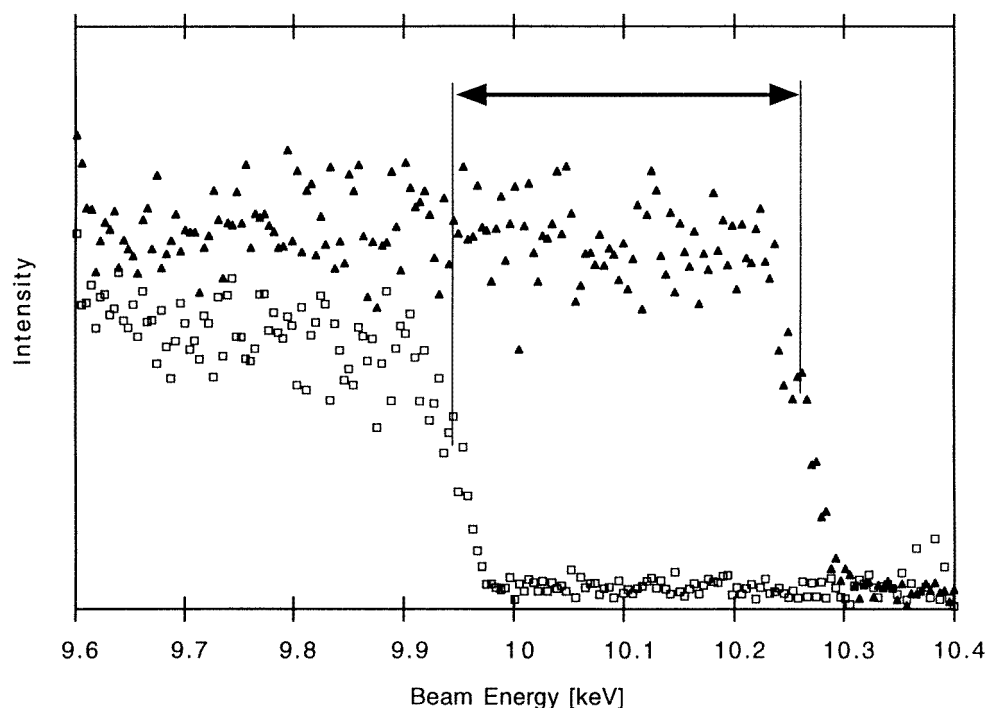


Figure 3. Intensities of photons due to radiative recombination into bare and hydrogen-like Ar as a function of electron beam energy. These spectra were derived from the data set shown in figure 2 using a fitting procedure described in the main text. The two-electron contribution to the ground state energy of helium-like argon is the interval indicated.

to the ground state energy of helium-like Ar. These calculations were performed using Cowan's Hartree-Fock plus relativistic corrections (HFR) code (Cowan 1981) and the general-purpose relativistic atomic structure program (Dyall *et al* 1989), which makes use of the relativistic Dirac-Fock (RDF) method.

In the HFR method, the major relativistic effects such as mass-velocity and Darwin terms are included directly in the non-relativistic Hartree-Fock equations. The Breit corrections are considered as a perturbation. In the RDF method, which is based on the Dirac-Coulomb Hamiltonian, all major relativistic effects are included automatically in Dirac-Fock equations. Higher-order QED contributions due to the transverse electromagnetic interaction and the radiative corrections are treated via perturbation theory. The HFR calculation gave a value of 303.342 eV whilst the RDF calculation gave a value of 303.366 eV. The tabulated values of binding energies for $1s_{1/2}$ hydrogen-like Ar (Johnson and Soff 1985) and $1s^2 \ ^1S_0$ helium-like Ar (Drake 1988) can also be used to arrive at the theoretical value of the two-electron contribution. This procedure gives a value of 305.56 eV. All the calculations differ from our measured value by about one standard deviation.

4. Discussion

We have measured the two-electron contribution directly for the ground state of helium-like Ar. The value obtained is in good agreement with previous calculations (Johnson and Soff 1985, Drake 1988) and our calculations presented above. The measurement technique used could be

applied to heavier ions, using a higher electron beam energy when it could provide a second-order test of two-electron QED effects directly (Persson *et al* 1996). For this measurement the Tokyo-EBIT (Currell *et al* 1996, Watanabe *et al* 1997a) is suitable. Due to the power-supply arrangement of this EBIT (Watanabe *et al* 1997b) it is possible to measure the differential electron beam energy scale directly with a high-accuracy voltmeter. This will then yield a high-accuracy value of the two-electron contribution of helium-like ions.

The essential idea behind this experiment is to measure an energy difference, with cancellation of many systematic errors. Below, we demonstrate the feasibility of such an experiment for krypton ions. The error of our present (absorption edge based) measurement is dominated by the error in determining the differential energy scale from the RR peaks. Using a super-EBIT, the main electron gun supply can be tuned to provide most of the beam energy whilst the small tunable portion is provided by a second power supply referenced to earth. A high-voltage voltmeter (1 kV range) attached directly to this second supply then provides the differential energy scale. Using such a setup, the error in the measurement presented above would have been 1.5 eV, dominated by the statistical quality of the data obtained in 20 h of beam time. Running for longer can further reduce this statistical error. For the same radiative recombination rate, about ten days of beam time would yield an uncertainty of 0.3 eV, constituting a second-order test of the two-electron Lamb shift (see the entry for $Z = 32$ in table 1 of Persson *et al*). Furthermore, increasing the electron-ion interaction rate by using higher current (beam currents in excess of 200 mA have been achieved with the Tokyo machine) or using a larger SSD may lead to a smaller final error.

There is still however one source of systematic error, which cannot be removed if the differential energy scale is measured directly with a voltmeter. The space charge of the electron beam acts to shift the energy scale in a way which depends on the electron beam energy. This effect occurs because a higher energy beam corresponds to a higher velocity and hence less charge per unit length for the same beam current.

The measured differential energy scale is defined with respect to the central drift tube wall. However, the electron interaction energy should be defined with respect to the electron beam. The difference between these energy scales is the average potential difference between the central drift tube and the electron beam (i.e. averaged over the electron beam profile). This difference in energy scale is given by

$$V_{sp} = V_0 \left\{ 2 \ln \left(\frac{r_{dt}}{r_e} \right) + \frac{1}{2} \right\} \quad (2)$$

where r_e is the electron beam radius, r_{dt} is the drift tube radius and V_0 is the potential experienced by ions on the edge of the electron beam due to its space charge. Herrmann theory (Herrmann 1958) predicts that the beam radius varies slowly as a function of electron beam energy having a value of about $30 \mu\text{m}$. Under the operating conditions of the present experiment, the term in curly brackets is constant with a value of about 10.5. If the beam was not tuned in the optimum way to be at the Herrmann radius, this value would be reduced so the following analysis gives an upper bound on the systematic error V_0 has a dependence on the beam energy, being given in volts by

$$V_0 \approx \frac{30I}{\sqrt{1 - \left(\frac{Ee}{511} + 1 \right)^{-2}}}. \quad (3)$$

Here I is the electron current in amps and Ee is the beam energy in kilovolts. Evaluating (2) and (3) at the two energies where the RR signal is attenuated by the absorption edge gives the maximum difference between the true energy difference and the measured energy difference (i.e. an upper bound on the systematic error). Under the present measurement conditions,

the difference in V_{sp} between the locations of the two absorption edges is about 1.8 V. The measurements presented here naturally take this systematic error into account since the electron energy scale was derived from the x-ray energy scale. If the energy scale was derived from a single low-voltage power supply (as proposed above), this systematic error would not be removed from the measurement. For example, the measurements for hydrogen-like and helium-like krypton presented by Currell *et al* (1999) suffer from this systematic error, with a magnitude of 0.21 V. It is interesting to note that this source of error reduces as the beam energy increases.

Preliminary experiments of this type have already been completed (Currell *et al* 1999). Analysis of the error budget associated with this measurement indicates that using about ten days of beam time should yield new benchmark values for the ground state two-electron contribution of helium-like krypton ions. Possible future refinements of this technique include retuning the EBIT to have a low beam current for a short measurement period (DeWitt 1992) to give a narrower electron beam energy spread and hence sharper features. This procedure would also reduce the systematic error due to space charge described above.

5. Conclusion

We have described a method for measuring the two-electron contribution of the ground state of helium-like ions, using an absorption edge as a low-pass x-ray energy spectrometer. We have used the technique to deduce the two-electron contribution for helium-like Ar and are currently extending the measurements to more highly charged ions, particularly helium-like krypton.

References

- Asada J *et al* 1997 *Phys. Scr.* T **73** 90–2
 Cowan R D 1981 *The Theory of Atomic Structure and Spectra* (Berkeley, CA: University of California Press)
 Currell F J *et al* 1996 *J. Phys. Soc. Japan* **10** 3186–92
 ——— 1997 *Phys. Scr.* T **73** 371–2
 Currell F J, Kato D, Nakamura N, Ohtani S, Sokell E J, Watanabe H and Yamada C 1999 *Phys. Scr.* T **80** 154
 Deutsch M and Hart M 1986 *J. Phys. B: At. Mol. Phys.* **19** L303
 DeWitt D R 1992 *PhD Thesis* Lawrence Livermore National Laboratory
 Drake G W 1988 *Can. J. Phys.* **66** 586
 Dyall K G, Grant I P, Johnson C T, Parpia F A and Plumer E P 1989 *Comput. Phys. Commun.* **55** 425
 Herrmann G J 1958 *Appl. Phys.* **29** 127
 Johnson W R and Soff G 1985 *At. Data Nucl. Data Tables* **33** 405
 Knapp D A 1991 *Z. Phys. D* **21** S143 (suppl.)
 Levine M A, Marrs R E, Bennet C L, Henderson J R, Knapp D A and Schneider M B 1989 *Int. Symp. on Electron Beam Ion Sources and Their Applications (AIP Conf. Proc. vol 188)* ed A Herschovitch (New York: AIP)
 Levine M A, Marrs R E, Henderson J R, Knapp D A and Schneider M B 1988 *Phys. Scr.* T **22** 157
 Margolis H S, Oxley P K, Varney A J, Groves P D and Silver J D 1997 *Phys. Scr.* T **73** 375
 Marrs R E, Elliot S R and Scofield J H 1997 *Phys. Rev. A* **56** 1338
 Marrs R E, Elliot S R and Stöhlker Th 1995 *Phys. Rev. A* **52** 3577
 Penetrante B M, Bardsley J N, DeWitt D, Clark M and Schneider D 1991 *Phys. Rev. A* **43** 4861
 Persson H, Salomonson S, Sunnergren P and Lindgren I 1996 *Phys. Rev. Lett.* **76** 204
 Press W H, Teukolsky S A, Vetterling W T and Flannery B P 1992 *Numerical Recipes in C: The Art of Scientific Computing* 2nd edn (Cambridge: Cambridge University Press)
 Silver J D *et al* 1994 *Rev. Sci. Instrum.* **65** 1072
 Stöhlker Th, Krämer A, Elliot S R, Marrs R E and Scofield J H 1997 *Phys. Rev. A* **56** 2819
 Watanabe H *et al* 1997a *J. Phys. Soc. Japan* **12** 3795
 ——— 1997b *Phys. Scr.* T **73** 365